

Novel synthesis of 3-(Phenyl) (ethylamino) methyl)-4-hydroxy-2H-chromen-2-one derivatives using biogenic ZnO nanoparticles and their applications



G.C. Anjan Kumar ^a, Yadav D. Bodke ^{a*}, B. Manjunatha ^a, N.D. Satyanarayan ^b, B.N. Nippu ^b, Muthipeedika Nibin Joy ^c

a: Department of PG Studies and Research in Chemistry, School of Chemical Sciences, Kuvempu University, 577451 Jnana Sahyadri, Shankaraghatta, Karnataka, India

b: Department of Pharmaceutical Chemistry, P.G. Centre, Kuvempu University, 577548 Katur, Karnataka, India

c: Innovation Centre for Chemical and Pharmaceutical Technologies, Institute of Chemical Technology, Ural Federal University, 620002 Mira st., 19, Yekaterinburg, Russia

* Corresponding author: ydbodke@gmail.com

This article belongs to the Regular Issue.

© 2021, The Authors. This article is published in open access form under the terms and conditions of the Creative Commons Attribution (CC BY) license (<http://creativecommons.org/licenses/by/4.0/>).

Abstract

The present work describes the novel synthesis of 3, 3'-((phenyl) (ethylamino) methyl)-4-hydroxy-2H-chromen-2-one derivatives catalyzed by biogenic ZnO nanoparticles. The synthesized heterocyclic compounds were characterized by fourier-transform infrared spectroscopy (FT-IR), nuclear magnetic resonance (NMR) and mass spectrometric techniques. Absorption, distribution, metabolism and excretion properties and various toxicities (ADMET) studies and *in silico* molecular docking studies were carried out for the synthesized compounds. The synthesized compounds were screened for their efficacy towards the antioxidant activity and were subjected to corrosion inhibition study towards the mild steel in acidic medium by weight loss method. Additionally, the recyclability of the employed catalyst was studied.

Keywords

MCRs
biogenic ZnO
benzylamino coumarins
antioxidant
corrosion inhibition

Received: 29.11.2021

Revised: 15.01.2022

Accepted: 15.01.2022

Available online: 21.01.2022

1. Introduction

In the past decades, the aqueous environment has elicited much consideration in organic synthesis. Water demonstrated unique reactivity and selectivity, which cannot be attained in conventional organic solvents [1]. Multicomponent reactions (MCRs) provide the most effective advance in the field of green chemistry and are vital tools in material, medical and modern synthetic organic chemistry; in particular, for the building of heterocyclic scaffolds. The last two decades were exclusively devoted to MCRs involving three or more precursors to synthesize structurally diverse bioactive heterocyclic compounds [2, 3]. The supremacy of MCRs are high atom-economy, convergence and structural diversity, operational simplicity of the resulting products makes this sustainable approach a potent tool for the synthesis of biologically active molecules and optimization processes in the medicinal industry [4-6]. Coumarin heterocyclic moiety is well regarded as a privileged structural motif in abundant natural products and

synthetic organic compounds of various pharmacological properties. The 4H-pyran core is a rich source of biologically vital molecules possessing a broad spectrum of biological and pharmacological activities [7]. Pharmacological activities includes neuroprotective agents [8], antimicrobial agents [9, 10], cardio preventive agents [11], antioxidant [12-14], anti-inflammatory agents [15] and antituberculating agents [16]. Further, the presence of N and O made them good corrosive inhibitors [17, 18]. Therefore, we tried to synthesize benzyl substituted coumarins via the Mannich type reaction. The Mannich reaction is one of the most powerful synthetic methods for carbon-carbon bond forming reactions for the synthesis of novel nitrogen-containing organic molecules.

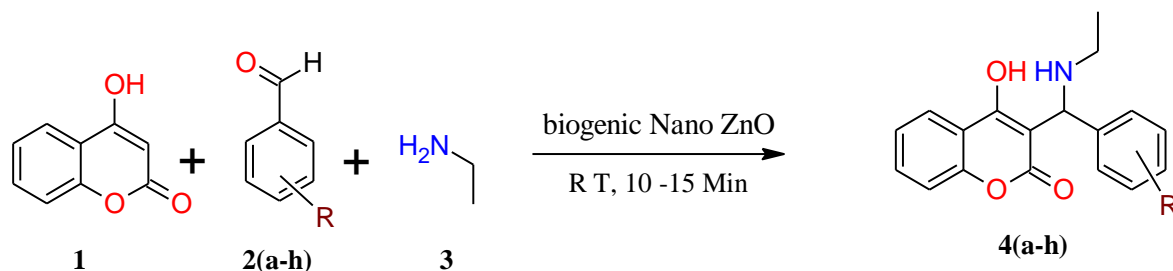
Currently, mild steel (MS) finds extensive applications in the industrial handling of alkali, acids, and salt solutions. The aggressiveness of these solutions causes brutal corrosion to engineered structures made of MS, which leads to immense economical and material losses. Hence, the study of MS corrosion and its inhibition has attracted

the attention of scientists and authorities to think up ways of overcoming the corrosion. Among the variety of corrosion control measures, utilization of corrosion inhibitors is a known method. It is identified that corrosion inhibitors act by adsorbing on the metal surface. Compounds having aromatic systems incorporated with N, S, and O heteroatoms have been found to possess exceptionally potent anticorrosion properties. In recent years, due to environmental issues, researchers have been functioning on the concept of diminished destructive effects to the environment to avoid the toxic effect of synthetic corrosion inhibitors [19–21].

In this regard, several methods have been employed for the synthesis of different corrosion inhibitors for the MS. Earlier methods employed for these types of synthesis suffered from many drawbacks such as poor yield, longer reaction time, use of expensive reagents, etc. One of the methods of overcoming these drawbacks is using the metal oxide nanoparticles as catalysts due to their higher surface-to-volume ratio of nanoparticles (NPs) which is predominantly responsible for their catalytic properties. In addition, they act as paramount adsorbents for the multitude of organic compounds, amplifying the reactivity of the reacting molecules [22, 23].

Synthesis of metal and oxide nanoparticles using plants and their parts is a sustainable method because of its environmental compatibility for pharmaceutical and other biomedical applications. Plants and their parts have emerged as a substitute to chemical synthetic procedures because no complex processes such as intracellular synthesis, no several purification steps are involved and no toxic chemicals are used in the synthesis. From the literature survey, among others, ZnO NPs have gained more attention because of their versatile characters like low toxicity, large surface area, high pore volume, low cost, Lewis acidic nature, ecofriendliness, heterogeneous nanocatalytic properties and reusability [24–26].

In the present study, we discussed the synthesis of 3-((phenyl) (ethylamino) methyl)-4-hydroxy-2H-chromen-2-one derivatives catalyzed by biogenic ZnO NPs by the reaction of 4-hydroxy coumarin with aromatic aldehydes and especially with ethylamine as an amine source. The schematic pathway is given in Scheme 1.



Where : R = 4-Cl, 4-NO₂, 3-NO₂, H, 4-OH, 3-OH, 4-OH 3-OCH₃, 4-OH 3-OCH₂CH₃.

Scheme 1 The schematic pathway of synthesis of 3-((phenyl) (ethylamino) methyl)-4-hydroxy-2H-chromen-2-one derivatives

2. Experimental

2.1. Materials and methods

All the chemicals were purchased from Sigma Aldrich, Merck and used as received with no further purifications. Areca nuts were collected from local suppliers near Chanagiri, Davanagere and used after washing with double distilled water. UV-Visible spectra were recorded using HR 4000 UV-Vis Spectrophotometer and FT-IR spectra by Alpha T Bruker instrument. The NMR spectra were recorded in DMSO with TMS as an internal standard on a Bruker Avance DRX 400 MHz spectrometer and chemical shift (δ) values were expressed in parts per million (ppm) units. High-resolution liquid chromatography-Mass Spectra (HRMS) were recorded using Water's SYNAPT G2 QTOF LCMS instrument, and the crystalline structure of ZnO was obtained by X-ray diffractometer (XRD) (Rigaku). The surface morphology and crystallinity were obtained by scanning electron microscopy (SEM), (CIIRC) and the elemental analysis of ZnO nanoparticles was conducted by energy dispersive analyzer using X-rays (EDX) (Thermo Scientific Noran 7). Molinspiration Cheminformatics web-based server [27] was used to evaluate drug likeliness; Absorption, distribution, metabolism and excretion properties and various toxicities (ADMET) prediction for all the designed compounds was evaluated using the ADMET descriptor module of the ADMET lab Web-based server [28]. Protein Used: Cyclooxygenase cox-2, Classification: Oxidoreductase and Organism(s): *Mus musculus*, PDB ID: 1PXX. *In silico* molecular docking study was also carried out by (ChemBioOffice Ultra 14.0 suite).

2.2. Preparation

2.2.1. Preparation of Areca nut extract mediated ZnO NPs

Freshly collected Areca nuts were stripped off their outer layer, washed with double distilled water, dried, and ground well to get a fine powder. To prepare the Areca nut extract, 5 g of Areca nut powder was boiled in water for about 30 min at 80 °C to get the reddish colour solution. Then the extract was filtered and dried under vacuum using a rotary evaporator.

The ZnO NPs were prepared by solution combustion method. In brief, 10 mL of Areca nut extract and 0.5 g of zinc nitrate hexahydrate $\text{Zn}(\text{NO}_3)_2 \cdot 6\text{H}_2\text{O}$ were weighed in a silica crucible and placed in a preheated muffle furnace maintained at 500 °C. An exothermic vigorous reaction leads to the formation of fine, white ZnO NPs. The obtained product was kept in a sealed container for further analysis [29].

2.3. Characterization of prepared nanomaterials

2.3.1. UV-Vis Spectroscopy

The UV-Vis absorption spectrum of ZnO nanoparticles was recorded between the wavelength of 200 and 800 nm and is presented in Fig. 1. The spectrum showed the absorbance peak at 293 nm corresponding to the characteristic band of zinc oxide nanoparticles. The bandgap energy (E) is calculated using the following equation:

$$E = \frac{hc}{\lambda}, \quad (1)$$

where h is the Planck constant, $6.626 \cdot 10^{-34}$ J·s, c is the velocity of light, $3.0 \cdot 10^8$ m/s, and λ is the wavelength (nm). The bandgap of ZnO NPs was found to be 3.15 eV.

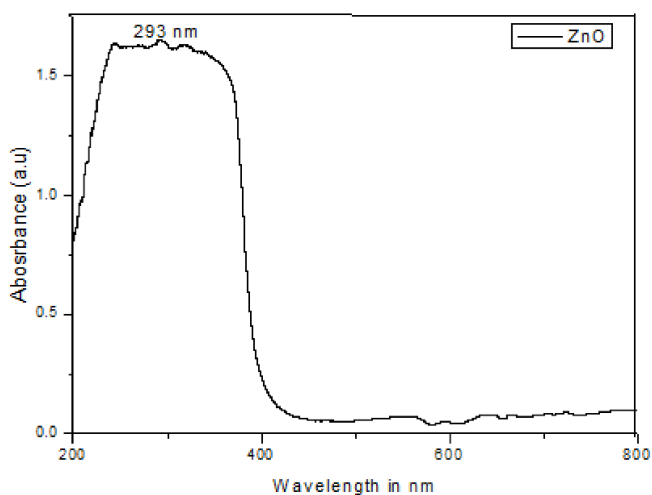


Fig. 1 UV-Vis Spectrum of ZnO NPs

2.3.2. FT-IR spectroscopy

The FT-IR spectrum of ZnO was recorded in the range of 400–4000 cm^{-1} and is presented in Fig. 2. The peaks at 3450.46 cm^{-1} and 1636.48 cm^{-1} are due to the stretching and bending vibration of the OH functionality. The peak at 1382.97 cm^{-1} is due to stretching vibrations of Zn–O–ZnO, and the peak between 700–400 cm^{-1} is due to stretching vibration of Zn–O.

2.3.3. X-Ray diffraction studies

The powder X-Ray Diffraction (P-XRD) pattern of prepared ZnO NPs is presented in Fig. 3. It indicates the phase purity and structural parameters of ZnO. The XRD peaks are observed in the wide-angle range of 2θ ($10^\circ < 2\theta < 80^\circ$).

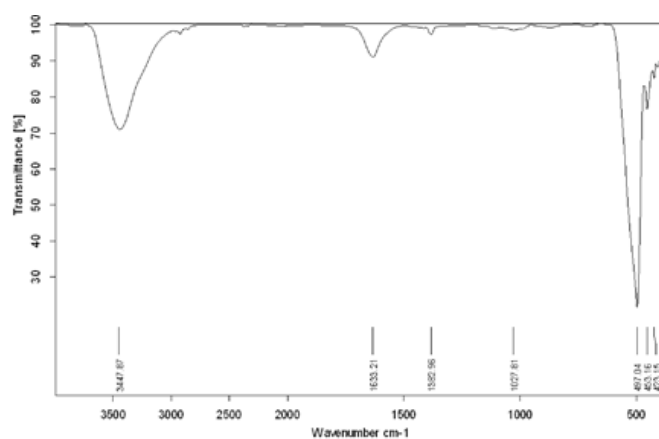


Fig. 2 FT-IR Spectrum of ZnO NPs

The reflections from (100), (002), (101) and (110) planes suggested that the synthesized nanoparticles possess hexagonal symmetry, which was further confirmed from the JCPDS No.: 01-089-0510. The crystallite size (D) can be determined by Scherrer's formula:

$$D = \frac{K\lambda}{\beta \cos\theta} \quad (2)$$

where λ is the wavelength of X-ray radiation ($\text{Cu K}\alpha = 0.15406$ nm), K is a constant taken as 0.90, β is the line width at half-maximum height (FWHM) of the peak and θ is the diffracting angle. The (100) plane is chosen to calculate the crystallite size. The average crystallite size for the synthesized ZnO NPs was found approximately 12 nm from this Debye-Scherrer equation 2.

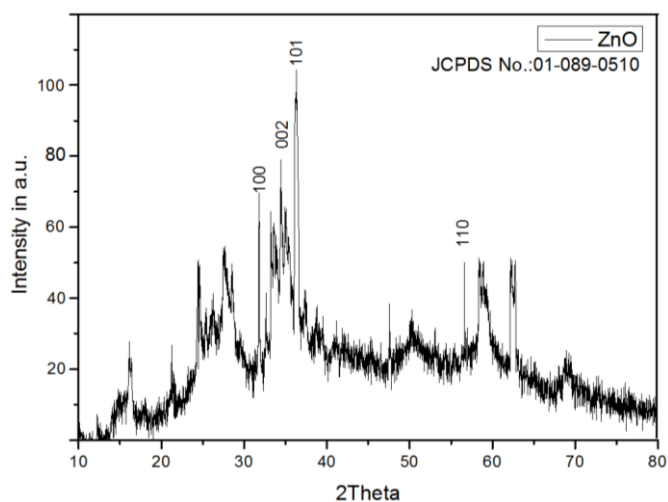


Fig. 3 XRD pattern of synthesized ZnO

2.3.4. SEM and EDX

The surface morphology of the prepared ZnO NPs was studied using scanning electron microscopic (SEM) technique; it showed that the particles were in spherical shape, as shown in Fig. 4. The Energy-dispersive X-ray spectroscopic (EDX) study was carried out for the prepared ZnO NPs to identify the elemental composition. EDX confirms the existence of zinc and oxygen signals of ZnO NPs as shown in Fig. 5.

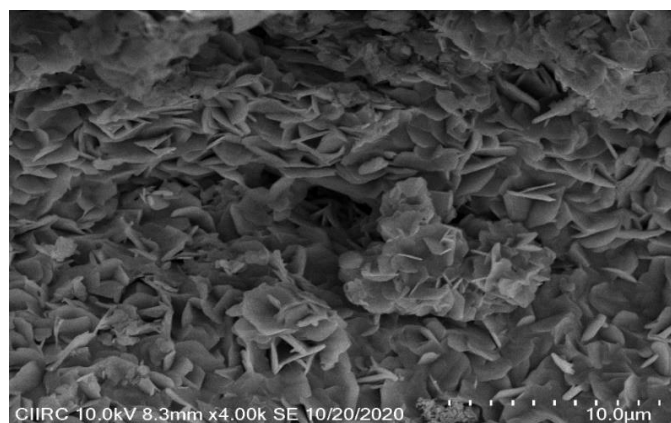


Fig. 4 SEM image of synthesized ZnO

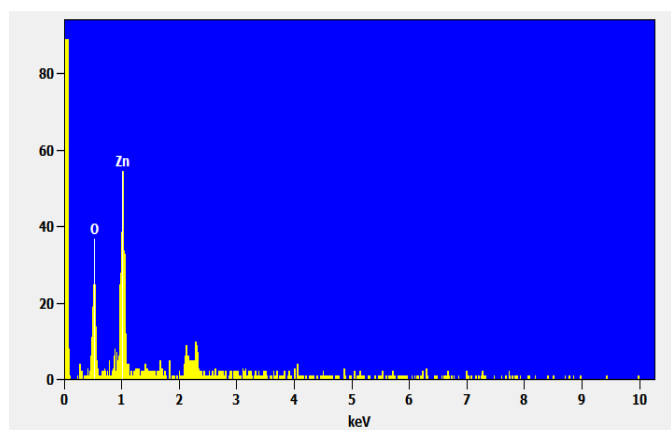


Fig. 5 EDX analysis of synthesized ZnO

The elemental analysis of the nanoparticle yielded 50.54% of zinc and 49.46% of oxygen, as shown in Table 1.

Table 1 The elemental analysis of synthesized nanoparticle

Element line	Weight %	Weight % error	Atom %	Atom % error
O	20.00	±1.43	50.54	±3.61
Zn	-	-	-	-
Zn	80.00	±3.36	49.46	±2.08
Total	100.00		100.00	

2.4. Synthetic procedure for 3-((phenyl) (ethylamino) methyl)-4-hydroxy-2H-chromen-2-one derivatives

A mixture of 4-hydroxy coumarin (1 mmol) **1**, aromatic aldehydes (1 mmol) **2**, ethylamine (1 mmol) **3**, and biogenic ZnO nanoparticles (5 mol.%) was taken in a round-bottom flask containing 10 mL water and stirred at room temperature. After the completion of the reaction (checked by thin-layer chromatography (TLC)), the reaction mixture was quenched in water, the solid compound obtained was filtered off, and the crude product was purified by recrystallization from EtOH.

2.4.1. 3-[(4-Chlorophenyl) (ethylamino) methyl]-4-hydroxy-2H-chromen-2-one: **4a**

White solid, Yield: 98%. m.p. 189–191 °C; FT-IR (KBr) in cm^{-1} : 3431 (O-H), 3137 (N-H), 2983 (Ar-H), 2708 (Aliphatic C-H) 1706 (C=O), 1604, 1518 (C-N), 756 (C-Cl). ^1H NMR (400 MHz, DMSO- d_6): δ : 10.20 (s, 1H, OH), 9.30 (s,

1H, NH), 8.54 (s, 1H, Ar-H), 8.22–8.20 (d, 1H, $J = 8.0$ Hz, Ar-H), 8.15–8.13 (d, 1H, $J = 8.0$ Hz, Ar-H) 8.01–7.99 (t, 1H, $J = 8.0$ Hz, Ar-H) 7.87–7.79 (m, 3H, Ar-H), 7.65–7.61 (t, 1H, $J = 8.0$ Hz, Ar-H), 7.55 (s, 1H, Ar-H), 7.51–7.40 (m, 1H, Ar-H), 5.52 (s, 1H, Aliphatic H), 2.95–2.65 (q, 2H, $J = 12.0$ Hz, CH_2), 1.19 (t, 3H, $J = 8.0$ Hz, CH_3) ppm. ^{13}C NMR (100 MHz, DMSO- d_6): 173.92 (C=O), 163.79, 154.23, 148.07, 147.33, 146.58, 141.39, 134.69, 131.44, 130.32, 128.83, 124.84, 123.25, 122.96, 116.37, 91.56, 58.35, 11.52 ppm. HRMS (ESI) $m/z = 330.06$ [M] $^+$; Mol. Formula: $\text{C}_{18}\text{H}_{16}\text{ClNO}_3$. Calcd: for C 65.56, H 4.89 and N 4.25. Found: C 65.60, H 4.90 and 4.20.

2.4.2. 3-[(Ethylamino) (4-nitrophenyl) methyl]-4-hydroxy-2H-chromen-2-one: **4b**

Yellow solid, 95%. m.p. 315–317 °C; FT-IR (KBr) in cm^{-1} : 3418 (O-H), 3063 (N-H), 2986 (Ar-H), 2803 (Aliphatic C-H) 1634 (C=O), 1602, 1519 (C-N), 1348 (N-O). ^1H NMR (400 MHz, DMSO- d_6): δ : 10.06 (s, 1H, OH), 9.98 (s, 1H, NH), 8.90 (s, 1H, Ar-H), 7.84 (d, 1H, 8.0 Hz, Ar-H), 7.62 (d, 2H, $J = 8.0$ Hz, Ar-H), 7.43–7.39 (t, 3H, Ar-H), 7.17–7.12 (q, 2H, $J = 8.0$ Hz, Ar-H), 5.34 (s, 1H, Aliphatic H) 2.92 (q, 2H, $J = 8.0$ Hz), 1.12 (t, 3H, $J = 7.9$ Hz, CH_3), ppm. ^{13}C NMR (100 MHz, DMSO- d_6): 173.83 (C=O), 163.75, 154.19, 138.29, 132.99, 131.31, 129.91, 128.70, 124.78, 123.93, 122.84, 122.57, 116.37, 91.96, 58.70, 11.53 ppm. HRMS (ESI) $m/z = 342.16$ [$\text{M}+1$]; Mol. Formula: $\text{C}_{18}\text{H}_{16}\text{N}_2\text{O}_5$. Calcd: for C 63.52, H 4.74 and N 8.23. Found: C 63.90, H 4.67 and 8.20.

2.4.3. 3-[(Ethylamino) (3-nitrophenyl) methyl]-4-hydroxy-2H-chromen-2-one: **4c**

Light yellow solid, Yield: 94%. m.p. 310–312 °C; FT-IR (KBr) in cm^{-1} : 3421 (O-H), 3067 (N-H), 2985, (Ar-H), 2808 (Aliphatic C-H) 1630 (C=O), 1606, 1524 (C-N), 1348 (N-O). ^1H NMR (400 MHz, DMSO- d_6): δ : 9.91 (s, 1H, OH), 9.06 (s, 1H, NH), 8.53 (s, 1H, Ar-H), 8.12 (d, 1H, $J = 12.0$ Hz, Ar-H), 7.99 (d, 1H, $J = 8.0$ Hz, Ar-H), 7.83–7.81 (t, 1H, $J = 7.9$ Hz, Ar-H), 7.62 (s, 1H, Ar-H), 7.40 (s, 1H, Ar-H), 7.13 (t, 2H, $J = 8.0$ Hz, Ar-H), 5.52 (s, 1H, Aliphatic CH), 2.95 (q, 2H, $J = 8.0$ Hz, CH_2), 1.19 (t, 3H, $J = 8.0$ Hz, CH_3) ppm. ^{13}C NMR (100 MHz, DMSO- d_6): 173.99 (C=O), 163.87, 154.32 148.15 141.49 134.80, 131.56, 130.44, 124.94, 123.37, 123.07, 122.66, 122.58, 116.49, 91.65, 58.38, 11.62, 1.70 ppm. HRMS (ESI) $m/z = 341.16$ [M] $^+$; Mol. Formula: $\text{C}_{18}\text{H}_{16}\text{N}_2\text{O}_5$. Calcd: for C 63.49, H 4.70, and N 8.23. Found: C 63.90, H 4.64 and 8.12.

2.4.4. 3-[(Ethylamino) (phenyl) methyl]-4-hydroxy-2H-chromen-2-one: **4d**

White solid, 93%. m.p. 274–276 °C; FT-IR (KBr) in cm^{-1} : 3419 (O-H), 3158, (N-H), 2981 (Ar-CH), 1634 (C=O), 1608, 1497 (C-N). ^1H NMR (400 MHz, DMSO- d_6): δ : 10.59 (s, 1H, OH), 9.42 (s, 1H, NH), 7.82–7.79 (q, 1H, $J = 8.0$ Hz, Ar-H), 7.59–7.56 (t, 2H, Ar-H), 7.31–7.25 (q, 3H, $J = 8.0$ Hz, Ar-H), 7.13–7.09 (m, 2H, $J = 8.0$ Hz, Ar-H), 5.28 (s, 1H, Aliphatic CH), 2.90 (q, 2H, $J = 7.2$ Hz, CH_2), 1.15 (t, 3H, $J = 8.0$ Hz, CH_3) ppm. ^{13}C NMR (100 MHz,

DMSO- d_6): 173.88 (C=O), 163.84, 154.26, 139.53, 131.36, 128.88, 128.48, 128.11, 124.84, 122.97, 122.68, 116.39, 92.28, 59.49, 11.63 ppm. HRMS (ESI) m/z = 296.11 [M]⁺; Mol. Formula: C₁₈H₁₇NO₃. C 73.20, H 5.80 and N 4.74. Found: C 75.40, H 5.90 and 4.70.

2.4.5. 3-[(Ethylamino) (4-hydroxyphenyl) methyl]-4-hydroxy-2H-chromen-2-one: 4e

White solid, 90% m.p. 245–247 °C; FT-IR (KBr) in cm⁻¹: 3409 (O-H), 3081 (N-H), 2987 (Ar-CH), 1638 (C=O), 1602, 1510 (C-N), 756. ¹H NMR (400 MHz, DMSO- d_6): δ : 9.74 (s, 1H, OH), 9.46 (s, 1H, NH), 8.92 (s, 1H, Ar-H), 7.82 (m, 1H, J = 12.0 Hz, Ar-H), 7.37–7.35 (d, 3H, J = 8.0 Hz, Ar-H), 7.12–7.10 (d, 2H, Ar-H), 6.69 (d, 2H, J = 8.4 Hz) 5.15 (s, 1H, Aliphatic CH), 2.88 (q, 2H, J = 8.0 Hz, CH₂), 1.14 (t, 3H, J = 12.0 Hz, CH₃) ppm. ¹³C NMR (100 MHz, DMSO- d_6): 173.89 (C=O), 163.84, 157.85, 154.24, 140.75, 131.36, 129.87, 124.83, 122.98, 118.73, 116.39, 115.46, 115.04, 92.21, 59.58, 11.64 ppm. HRMS (ESI) m/z = 311.09 [M]⁺; Mol. Formula: C₁₈H₁₇NO₄. Calcd. for C 69.44, H 5.50 and N 4.50. Found: C 69.49, H 5.44 and 4.46.

2.4.6. 3-[(Ethylamino)(3-hydroxyphenyl) methyl]-4-hydroxy-2H-chromen-2-one: 4f

White solid, 91% m.p. 237–239 °C; FT-IR (KBr) in cm⁻¹: 3452 (O-H), 3108 (N-H), 2875 (Ar-CH), 1649 (C=O), 1616, 1516 (C-N). ¹H NMR (400 MHz, DMSO- d_6): δ : 10.31 (s, 1H, OH), 9.47 (s, 1H, NH), 8.83 (s, 1H, J = 7.6 Hz, Ar-H), 7.88 (d, 1H, J = 8.0 Hz, Ar-H), 7.48 (m, 1H, Ar-H), 7.22–7.14 (m, 3H, J = 8.0 Hz, Ar-H), 7.07 (q, 2H, J = 7.9 Hz), 6.72–6.70 (t, 1H, Ar-H), 5.25 (s, 1H, Aliphatic H), 2.96–2.91 (q, 2H, J = 7.2 Hz, CH₂), 1.22 (t, 3H, J = 7.2 Hz, CH₃) ppm. ¹³C NMR (100 MHz, DMSO- d_6): 173.34 (C=O) 163.27 157.30, 153.69, 140.18, 130.77, 129.29, 124.26, 122.39, 118.19, 115.82, 115.41, 114.92, 114.50, 91.64, 59.12, 11.09 ppm. HRMS (ESI) m/z = 311.97 [M]⁺; Mol. Formula: C₁₈H₁₇NO₄. Calcd. for C 69.44, H 5.50, and N 4.50. Found: C 69.40, H 5.54 and 4.43.

2.4.7. 3-[(Ethylamino) (4-hydroxy-3-methoxyphenyl) methyl]-4-hydroxy-2H-chromen-2-one: 4g

White solid, 90% m.p. 235–237 °C; FT-IR (KBr) in cm⁻¹: 3435 (O-H), 3098 (N-H), 2856 (Ar-CH), 1649 (C=O), 1606, 1539 (C-N). ¹H NMR (400 MHz, DMSO- d_6): δ : 10.07 (s, 1H, OH), 9.05 (s, 1H, NH), 8.72 (s, 1H, Ar-H), 7.88 (d, 1H, J = 8.0 Hz, Ar-H), 7.48–7.44 (m, 1H, Ar-H), 7.27 (d, 1H, J = 2.0 Hz, Ar-H), 7.21–7.15 (m, 2H, J = 7.8 Hz, Ar-H), 7.00 (d, 1H, J = 8.0 Hz, Ar-H), 6.71 (d, 1H, Ar-H), 5.22 (s, 1H, Aliphatic CH), 3.76 (s, 3H, CH₃), 2.92–2.87 (q, 2H, J = 7.8 Hz, CH₂), 1.21 (t, 3H, J = 12.0 Hz, CH₃) ppm. ¹³C NMR (100 MHz, DMSO- d_6): 173.29 (C=O), 163.31, 153.67, 152.84, 147.25, 146.55, 130.68, 129.63, 124.28, 122.34, 120.57, 115.78, 115.08, 112.40, 92.00, 59.13, 55.69, 11.10 ppm. HRMS (ESI) m/z = 341.09 [M]⁺; Mol. Formula: C₁₉H₁₉NO₅. Calcd. for C 66.85, H 5.61 and N 4.10. Found: C 66.80, H 5.56 and 4.06.

2.4.8. 3-[(3-Ethoxy-4-hydroxyphenyl) (ethylamino) methyl]-4-hydroxy-2H-chromen-2-one: 4h

White solid, 90% m.p. 288–290 °C; FT-IR (KBr) in cm⁻¹: 3452 (O-H), 3111 (N-H), 2856 (Ar-CH), 1649 (C=O), 1632, 1513 (C-N). ¹H NMR (400 MHz, DMSO- d_6): δ : 10.04 (s, 1H, OH), 8.99 (s, 1H, NH), 8.77 (s, 1H, Ar-H), 7.89 (d, 1H, J = 8.0 Hz, Ar-H), 7.48 (t, 1H, J = 7.90 Hz, Ar-H), 7.27 (s, 1H, Ar-H), 7.21–7.15 (q, 2H, J = 8.0 Hz, Ar-H), 7.00 (d, 1H, J = 8.0 Hz, Ar-H), 6.76 (s, 1H, J = 8.0 Hz, Ar-H), 5.22 (s, 1H, Aliphatic CH), 4.03–3.97 (q, 2H, J = 8.0 Hz, CH₂), 2.93–2.87 (q, 2H, J = 8.0 Hz, CH₂), 1.35–1.31 (t, 3H, J = 8.0 Hz, CH₃), 1.22 (t, 3H, J = 8.0 Hz, CH₃), ppm. ¹³C NMR (100 MHz, DMSO- d_6): 173.28 (C=O), 163.33, 153.67, 152.45, 146.89, 146.38, 130.69, 129.63, 124.29, 122.36, 120.65, 115.79, 115.18, 113.81, 92.07, 64.08, 59.06, 14.76, 11.10 ppm. HRMS (ESI) m/z = 340.09 [M]⁺; Mol. Formula: C₂₀H₂₁NO₅. Calcd. for C 67.59, H 5.96 and N 3.94. Found: C 67.53, H 5.90 and 3.92.

3. Results and discussion

3.1. Chemistry

The structure of synthesized compounds was characterized by using different spectroscopic techniques such as UV-Vis, FT-IR, ¹H NMR, ¹³C NMR and HRMS. The FT-IR spectrum of the compound **4a** showed strong absorption bands at 756 cm⁻¹ due to the chlorine atom attached to the benzene ring, 1529 cm⁻¹ and 1518 cm⁻¹ due to C-N, 1706 cm⁻¹ due to C=O functionality of coumarin ring, 2708 cm⁻¹ due to aliphatic -CH, 2983 cm⁻¹ due to aromatic CH, 3137 cm⁻¹ due to N-H and 3431 cm⁻¹ due to -OH functionality. The ¹H NMR spectrum of the compound **4a** showed a singlet at δ 10.20 due to the OH proton and another singlet at δ 9.30 ppm due to the NH proton. The multiplet appeared between δ 7.12–8.50 ppm is due to the presence of aromatic protons. It also displayed a singlet at δ 5.50 ppm due to the -CH proton. In the HRMS spectrum of the compound **4a**, it showed a molecular ion peak M⁺ at m/z 330.0664, which is close to its molecular weight.

The reaction of 4-hydroxy coumarin (**1**), aromatic aldehyde (**2(a-h)**), and ethylamine (**3**) achieved the desired product 3-((phenyl) (ethylamino) methyl)-4-hydroxy-2H-chromen-2-one (**4(a-h)**) by using biogenic ZnO NPs in green solvent (Scheme 1).

Initially, to come across the finest conditions, screening was performed with solvent-free and a variety of polar and nonpolar solvents like DMSO, DMF, ethanol, methanol, toluene, tetrahydrofuran, acetonitrile, ethanol, methanol, polyethylene glycol and water, as shown in Table 2. We observed that the polar protic solvents afforded better yield than other solvents, and in water (Table 2, Entry 11) the supreme catalytic activity of biogenic nano ZnO was observed.

Further, we were concentrated on the efficient assessment of various catalysts for the model reaction in an aqueous medium at room temperature.

Table 2 Effect of solvents on the three-component synthesis of benzylamino coumarin derivative **4a**

Entry	Solvents	Yield ^a (%)
1	No solvent	–
2	Toluene	43
3	Tetrahydrofuran	46
4	Acetonitrile	54
5	DMSO	63
6	DCM	61
7	DMF	56
8	Ethanol	79
9	Methanol	75
10	Polyethylene glycol (PEG)	80
11	H ₂ O	98

^a Isolated yield

A wide variety of catalysts, including L-proline, alum, tetrabutylammonium bromide, nano aluminum oxide (Al₂O₃), zeolites, bulk ZnO and biogenic ZnO NPs, were employed to study their efficacy for the synthesis of benzyl amino coumarins. 68% yield of product was obtained in 4 h by using bulk ZnO and the results are presented in Table 3 which illustrates that the presence of biogenic nano ZnO has given the products with 98% yield within 10–15 min. Therefore, this catalyst appeared to be of better quality than any of the other catalysts.

Table 3 Influence of different catalysts on the synthesis of benzylamino coumarin derivative **4a**

Entry	Catalysts	Time (h)	Yield ^a (%)
1	L-proline	6.0	45
2	Alum	8.0	30
3	Acetic acid	4.5	60
4	Bi(NO ₃) ₃ ·5H ₂ O	1.45	94
5	Tetrabutylammonium	6.0	25
6	Nano aluminium oxide	8.0	26
7	Zeolites	7.0	35
8	Bulk ZnO	4.0	68
9	Biogenic ZnO NPs	10–15 min	98

^a Isolated yield

After the selection of catalyst, we have concentrated on the amount of the catalyst to be used by varying the mole ratio of the biogenic ZnO NPs. Table 4 displays the different mole ratios of catalyst employed on the model reaction. It shows unambiguously that the enhancement of catalyst load from 3 to 15 mol.%, amplified the yield of the desired product to a large extent (38–98%).

Table 4 Optimization of catalyst loading on model reaction

Entry	Catalysts	Yield ^a (%)
1	Nano-ZnO (3 mol.%)	38
2	Nano-ZnO (5 mol.%)	98
3	Nano-ZnO (7 mol.%)	92
4	Nano-ZnO (10 mol.%)	90
5	Nano-ZnO (15 mol.%)	85
6	Nano-ZnO (5 mol.%) + L-Proline	65
7	Nano-ZnO (5 mol.%) + p-toluenesulphonic acid (5 mol.%)	15
8	Nano-ZnO (5 mol.%) + Methanesulphonic acid (5 mol.%)	29
9	Nano-ZnO (5 mol.%) + boric acid (5 mol.%)	25
10	Nano-ZnO (5 mol.%) + Tetrabutylammonium bromide (5 mol.%)	30

^a Isolated yield of the pure product

Again, it also observed that no other additive combinations like protic or lewis acids are at all beneficial in this method.

These groundwork results encouraged us to advance the applicability of the catalyst for the synthesis of coumarin derivatives. To study the possibility and limitations of this protocol, we engaged a series of aromatic aldehydes with ethylamine to get the resultant BAC. In view of these results, we propose a mechanistic interpretation for the high catalytic activity of biogenic nanocrystalline ZnO, especially in aqueous media. The nano ZnO catalyst-water colloidal combination plays vital accountability for the swift formation and stabilization of the imine intermediate. The catalyst may encourage 4-hydroxy coumarin to act as the Mannich donor for the rapid formation of benzylamino coumarin derivatives. The swift imine generation and subsequent C–C bond development within a very little instant catalyzed by amphoteric nano ZnO (colloidal composite) are the striking features of this protocol.

To generalize this method, the reaction was studied using different aromatic aldehydes and the results are appended in Table 5. Aromatic aldehydes with different substitutions underwent smooth reactions with ethylamine and 4-hydroxycoumarin, furnishing the respective products in good yields and considerably shortened reaction time in comparison with the previously reported methods. However, under the same conditions, when the aliphatic aldehydes were used as starting materials, for up to 12 h we could not observe any products, but after 14 h, traces of biscoumarin were observed.

Table 5 Optimization of the model reaction

Entry	Aldehyde	Amine	Product	Time (min)	Yield ^a %	M.P. (°C)
1	4Cl	CH ₃ CH ₂ NH ₂	4a	15	98	189–191
2	4-NO ₂	CH ₃ CH ₂ NH ₂	4b	10	95	315–317
3	3-NO ₂	CH ₃ CH ₂ NH ₂	4c	10	94	310–312
4	H	CH ₃ CH ₂ NH ₂	4d	15	93	274–276
5	4-OH	CH ₃ CH ₂ NH ₂	4e	15	90	245–247
6	3-OH	CH ₃ CH ₂ NH ₂	4f	10	91	237–239
7	4-OCH ₃	CH ₃ CH ₂ NH ₂	4g	10	90	235–237
8	4-OH, 3-OCH ₃	CH ₃ CH ₂ NH ₂	4h	15	90	288–290

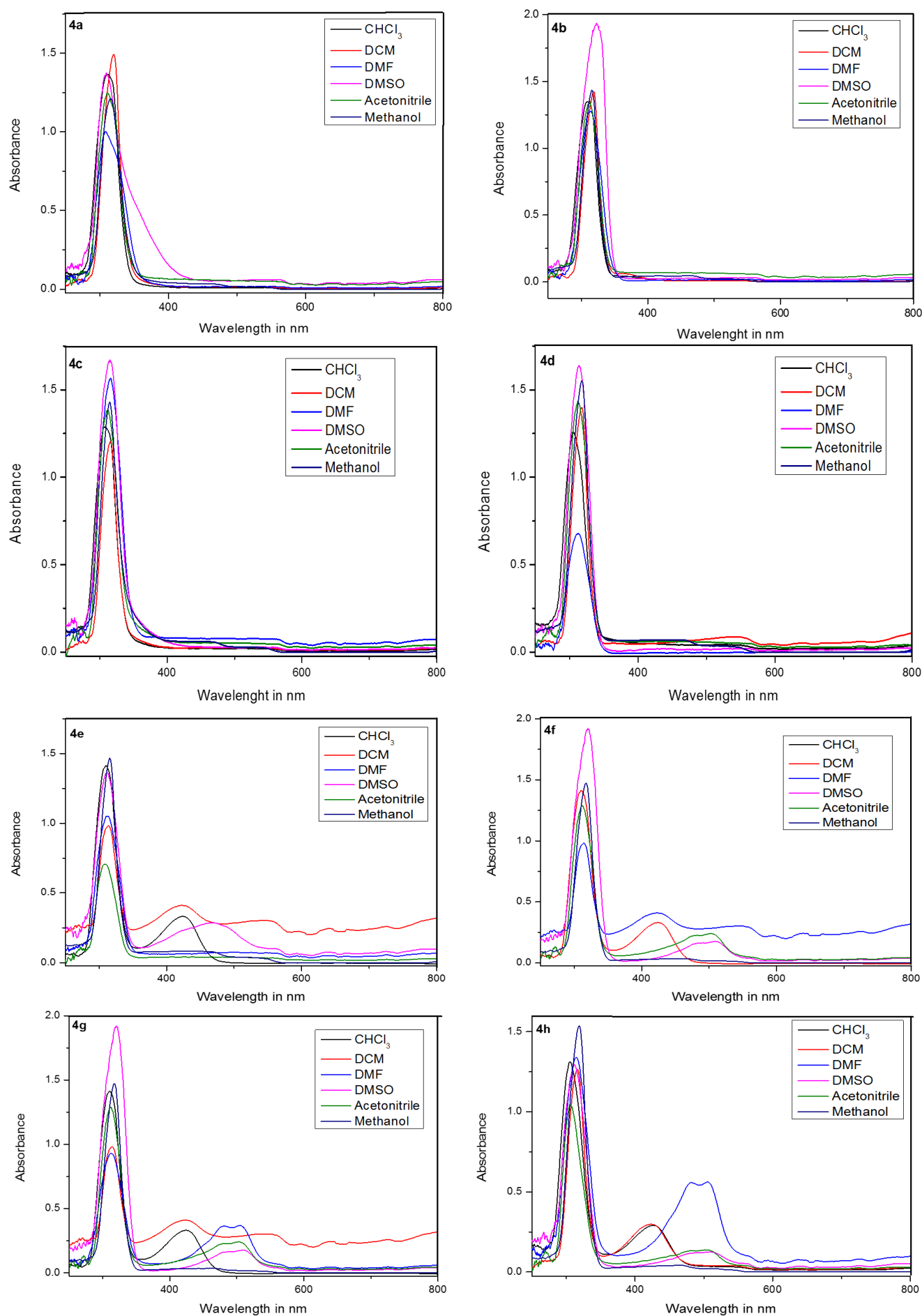


Fig. 6 Electronic spectra of synthesized compounds in different solvents

Further, the same reaction was performed using aromatic amines, but no detectable products were obtained and this may be due to the low solubility of aromatic amines in water.

3.2. Absorption studies

The UV-Vis absorption spectra of compounds **4(a-h)** were recorded in various solvents and the effect of solvent polarity and the electronic substitution were studied at a concentration of 10^{-5} M at room temperature. The typical absorption spectra are displayed in Fig. 6. The absorption maxima (λ_{\max}) and its corresponding logarithmic molar extinction coefficient (intensity of the absorption) for all the compounds in studied solvents were obtained from the plot and summarized in Table 6 and Table 7, respectively. The electronic spectra of the synthesized compounds **4(a-h)** showed broad peaks in the region 300–325 nm due to $\pi \rightarrow \pi^*$ transitions respectively and additional peaks from 420–510 nm appeared in these compounds were owing to the interaction of attached electron-donating groups (4-OH, 3-OH, OCH₃, and 4-OH OCH₃) with polar solvent due to $n \rightarrow \pi^*$. From the close examination of the spectral data (Table 6), it can be noted that as the solvent polarity increases, the absorption maxima shift towards a longer wavelength so that the bathochromic shift is observed in all the compounds. This may be due to the effective interaction between the solvent molecules and the lone pair of electrons present on the electron-donating sites of synthesized compounds. The presence of electron-donating substituents on the aromatic ring group also contributes to the bathochromic shift. This study concludes that solvent polarity and electronic substitution played a very important role in the shift of λ_{\max} for all the studied compounds.

Table 6 The electronic spectral data of the compounds (**4(a-h)**) in different solvents

Compounds	λ_{\max} (nm)					
	CHCl ₃	DCM	DMF	DMSO	ACN	MeOH
4a	312	317	306	310	312	314
4b	309	317	314	321	312	316
4c	308	315	316	316	311	315
4d	306	317	311	314	311	316
4e	310	311	311	311	308	315
4f	308	310	311	319	308	315
4g	308	314	312	320	312	315
4h	306	315	314	312	312	317

3.3. *In silico* molecular docking studies

3.3.1. Drug Likeness (Molinspiration Physicochemical Parameters)

Molinspiration software was used to predict the physicochemical parameters of synthesized compounds **4(a-h)** like drug-likeness activities and it is used to make sure whether the synthesized compounds are alike to existing drugs. Drug-likeness measurements were governed by the famous rule called Lipinski's rule of five and drug-likeness data were useful to study the pharmacokinetic

parameters like absorption, distribution, metabolism, and excretion from the living body [30, 31]. The computed values are tabulated in Table 8. All the compounds exhibited fine physicochemical parameters: enough number of rotational bonds, which would illustrate good flexibility. Further, the ample number of H-donors and H-bond acceptors of the synthesized compounds exhibited strong binding with target molecules. The good absorption values from computed data uncovered by all the synthesized compounds and so can easily be absorbed by the living systems. The % ABS was calculated by using the formula % ABS = 109 - (0.345 x TPSA). All the synthesized compounds showed good absorption, i.e., % ABS = 60.5482–76.3561 which ranges from considerable to good range. Also, we calculated the hydrophilicity values of the octanol-water partition coefficient (milogP), which indicates toxicity, absorption, and drug-receptor interactions. The data range of milogP for the synthesized compounds is from 1.05 to 2.19. This range is less than 5.0 and showed good concurrence as per Lipinski's rule. Also, the number of H-bond acceptors ranges from 2–5 for synthesized compounds that are less than 10, and the number of H-bond donors for all synthesized compounds is 2 and thus, less than 5 as per the rule. According to the Lipinski (Pfizer's rule) of five for any chemical compound, as an oral drug would be biologically active if it does not violate more than one rule out of the proposed rules wherein, the first rule said, the octanol-water partition coefficient (milogP) must be ≤ 5 ; the second rule said, the molecular weight of the probable drug must be < 500 Daltons; the third rule said, taking into consideration of the number of H-bond acceptors in the molecule under consideration must be ≤ 10 and the last rule said, the number of H-bond donors must be ≤ 5 [32, 33]. Table 9 disclosed bioactivity results, showing that the parameters of all the synthesized compounds were within limits of Lipinski's rule of five with no violation of rules. Thus, all the synthesized molecules **4(a-h)** possessed good drug-like properties.

3.3.1.1. ADMET Studies

ADMET prediction for all the designed compounds was evaluated using the ADMET descriptor module of the ADMET lab Web-based server [34]. Various ADME descriptors like LogS, LogP, intestinal absorption, Caco-2 Permeability, Plasma Protein binding Percentage, CNS Blood-Brain Barrier, cytochrome P450 models, and toxicity descriptors like Hepatotoxicity, Mutagenicity, LD₅₀ value, Half-life and Clearance of the drug were used to predict properties related to pharmacokinetics.

The synthesized compounds were subjected to study their toxicity before their application. All of them moderately toxic, having a lower value of LD₅₀ compared to the standard (LD₅₀ < 500 mg/kg indicate high toxicity, LD₅₀ 500 to 1000 mg/kg indicates reasonable toxicity, LD₅₀ 1000 to 2000 mg/kg shows low toxicity). The LD₅₀ values are listed in Table 10.

Table 7 logarithmic molar extinction coefficient of studied compounds **4(a-h)**

Compounds	Logarithmic molar extinction coefficient (L M ⁻¹ cm)					
	CHCl ₃	DCM	DMF	DMSO	ACN	MeOH
4a	6.1373	6.1781	6.0047	6.1401	6.0955	6.0812
4b	6.1586	6.1522	6.1078	6.2848	6.1251	6.1303
4c	6.1565	6.0820	6.1945	6.2219	6.1115	6.1414
4d	6.0996	6.1473	5.8356	6.2151	6.1878	6.1559
4e	6.1705	5.9934	6.0224	6.1338	5.8509	6.1489
4f	6.1728	6.1489	5.9925	6.2798	6.1065	6.0989
4g	5.9929	5.9929	5.9661	6.2846	6.1061	6.1075
4h	6.1051	6.1051	6.1287	6.1120	6.1146	6.1146

Table 8 Drug-likeness results of the synthesized compounds **4(a-h)**

Compound	MW g/mol	logP	nHA	nHD	TPSA	nViolations
4a	329.080	3.465	4	2	62.470	0
4b	340.110	2.634	7	2	105.610	0
4c	340.110	2.617	7	2	105.610	0
4d	295.120	2.633	4	2	62.470	0
4e	311.120	2.903	5	3	82.364	0
4f	311.337	2.903	5	3	82.723	0
4g	341.363	2.912	6	3	91.931	0
4h	355.391	3.302	6	3	91.931	0

Table 9 ADMET results of the synthesized compounds **4(a-h)**

Ligands	^a LogS (Log mol/l)	^b PCaco (cm/s)	^c Intestinal absorption(HIA) in %	^d logPGI (inhibitor)	^e logPGI Substrate	^f logBB Probability	^g Plasma protein binding in %	^h CYP450 2D6 inhibitor	ⁱ P450 CYP2D6 substrate
4a	-3.469	-4.930	63.1	NI	NS	0.896	95.668	NI	NS
4b	-3.370	-4.953	45.8	NI	NS	0.773	95.378	NI	NS
4c	-3.198	-4.975	45.8	NI	NS	0.696	93.374	NI	NS
4d	-2.881	-4.930	60.0	NI	NS	0.888	91.289	I	NS
4e	-2.781	-5.004	40.5	NI	NS	0.735	93.256	NI	NS
4f	-2.624	-5.079	44.5	NI	NS	0.656	85.096	NI	NS
4g	-2.800	-5.036	34.9	NI	NS	0.676	87.738	I	NS
4h	-3.083	-4.949	29.2	NI	NS	0.593	91.268	NI	NS
Ibuprofen	-3.736	-4.379	85.7	NI	NS	0.991	87.592	NI	NS

^a Predicted aqueous solubility (Optimal level - higher than - 4 log mol/L); ^b Predicted Caco-2 cell permeability (cm/s) (Optimal level higher than -5.15); ^c Predicted Human intestinal absorption in % (acceptable level $\geq 30\%$); ^d Predicted P-glycoprotein inhibitor (I - Inhibitor, NI - Non Inhibitor); ^e Predicted P-glycoprotein substrate (S - Substrate, NS - Non-substrate); ^f Blood/brain barrier probability (acceptable value ≥ 0.1 is acceptable, < 0.1 is poor); ^g Plasma protein binding (optimal level greater than 90% drugs that are highly protein-bound and have a low therapeutic index); ^h CYP450 2D6 inhibitor (I-Inhibitor, NI-Non-Inhibitor); ⁱ P450 CYP2D6 substrate (S - Substrate, NS - Non-substrate).

Table 10 Toxicity evaluation designed molecules **4(a-h)**

Ligands	^a T _{1/2} half life (h)	^b Clearance (L/min/kg)	^c LD ₅₀ (mg/kg)	^d Human Hepatotoxicity	^e AMES toxicity
4a	1.910	1.690	811.387	Yes	No
4b	1.625	1.753	911.815	Yes	Yes
4c	1.564	1.754	790.509	Yes	Yes
4d	2.070	2.078	708.467	Yes	No
4e	1.760	2.348	692.199	Yes	No
4f	2.249	2.324	658.007	Yes	No
4g	1.578	2.086	616.902	Yes	No
4h	1.690	2.140	577.704	Yes	No
Ibuprofen	0.801	0.536	2555.452	Yes	No

^a Half life in hour (Optimal level > 0.5 h, > 8 h - high, < 3 h - low); ^b Clearance of drug in mL/min/kg (> 15 mL/min/kg - high; 5 mL/min/kg < 15 mL/min/kg - moderate; < 5 mL/min/kg - low); ^c LD₅₀ Oral Rat Acute Toxicity in Mol/kg; ^d Human hepatotoxicity (Yes - Hepatotoxic, No - Nonhepatotoxic); ^e AMES Mutagenicity (Yes - Mutagenic, No - Non-mutagenic).

After the determination of cytotoxicity and an *in silico* molecular docking, the study was carried out with cyclooxygenase cox-2 to learn the interaction and binding mode with different amino acids, the binding energy, number of hydrogen bonds, and hydrophobic interactions, docking scores (affinity) were compared with the diclofenac. The molecular docking results of synthesized compounds are given in Table 11. From the *in silico* studies, it was confirmed that all the studied compounds **4(a-h)** have the most similar binding energy compared to diclofenac. The most potent cytotoxic compound **4f** has a strong binding affinity (-9.3 kcal/mol) which is equal to the binding energy of diclofenac sodium by forming one hydrogen bond with SER530. Fig. 7-9 shows the 2D and 3D representation of the interaction of synthesized compounds **4(a-h)** and standard Diclofenac drug.

3.3.1.2. Preparation of ligand

The structure of ligands was drawn using ChemDraw software and the build of 3D structure and energy of each ligand was minimized using the USCF chimera tool by applying the AMBER force field and then ligands were converted into PDB format.

3.3.1.3. Preparation of the receptor

The crystal structure of diclofenac bound to the cyclooxygenase active site of cox-2 PDB ID: 1PXX [35] was accessed through a protein data bank [36]. The co-crystal structures of proteins and water molecules are removed from proteins. With the addition of hydrogen, merging of non-polar hydrogen, adding charges, and energy minimization of proteins by an AMBER force field carried out by using the USCF chimera tool, prepared proteins were transformed into PDB format.

3.3.1.4. Grid box selection

Based on the active site and binding site TYR385, HIS07, TYR55 and ARG120 grid boxes were arranged.

3.3.1.5. Docking and visualization

The setting of a grid box around the active sites of proteins, designed ligands were docked against the receptor using Autodock Vina in the PyRX workstation. The Autodock Vina docking algorithm has been used to search for the best-docked ligand and target conformation. Ligands with the lowest binding affinity were considered as the best conformation, docked protein and target were converted into PDB format by Schrodinger PyMol, and interactions - visualized Biovia Discovery studios [37-40].

The structure of the protein used is given in Fig. 10.

All the docking results of ligand molecules showed potential ligand affinity. Amongst the docked molecules in complex with cyclooxygenase cox-2, the compounds **4b**, **4h** and **4g** were found to have the best dock confirmation with a maximum binding affinity (-8.0, -8.0 and -8.1 kcal/mol); the compound **4b** establishes four hydrogen bonds and the compound **4h** exhibits two hydrogen bond with the active enzymatic sites. Also, the compounds **4a** and **4h** showed a more hydrophobic interaction with the tested protein compared to the standard. The compounds **4d**, **4g** and **4h** have electrostatic interactions. Concerning *in silico*, all eight compounds showed good hydrophobic interactions with the binding affinity values ranging between 8.0-9.3 kcal/mol against the amino acid molecules regarding the cyclooxygenase cox-2 synthase protein.

Table 11 Docking results of ligands with Cyclooxygenase cox-2

Ligand	Binding affinity (kcal/mol)	Hydrogen bond interaction	Hydrogen Bond length in Å	Electrostatic interaction	Hydrophobic and Other interactions
4a	-8.7	SER530, GLY526	2.06, 3.64	-	VAL349, ALA526, VAL116, TYR385, VAL523, LEU352, TRP387, PHE518, LEU359, SER532, TYR348, TYR355, MET13
4b	-8.0	HIS90, PHE518, SER353, SER530	2.66, 2.69, 2.84, 3.31	-	VAL523, TYR355, LEU359, VAL349, LEU352, ALA527, ARG513, PHE381, TYR385, ARG120, GLY526
4c	-8.6	TYR355	2.14	-	VAL523, LEU531, VAL349, SER530, ARG513, ALA527, HIS90, PHE518, TYR385
4d	-8.8	SER530, SER353	2.39	MET522	TRP387, ALA527, LEU357, TYR348, VAL344, LEU352, ARG120, GLY526, TYR385
4e	-8.8	SER530	2.22	-	VAL349, TRP387, ALA527, LEU357, TYR348, VAL344, LEU351, VAL523
4f	-9.3	SER530	2.32	-	VAL349, TRP387, ALA527, LEU357, TYR348, VAL344, LEU351, VAL523
4g	-8.1	SER530, VAL523, MET522	2.61, 3.1, 3.33	MET113	LEU359, ALA527, VAL116, LEU531, LEU532, TYR385, TRP387, PHE518, TYR355, ARG120
4h	-8.0	SER530, VAL523	2.69, 3.20	MET113	LEU359, ALA527, VAL116, LEU531, LEU532, TYR385, TRP387, PHE518, TYR355, ARG120, GLY526, PHE381
Diclofenac	-9.3	TYR385, SER530	2.73, 2.65	-	ALA527, VAL349, TYR348, VAL523, LEU351, PHE381, TRP387, GLY526

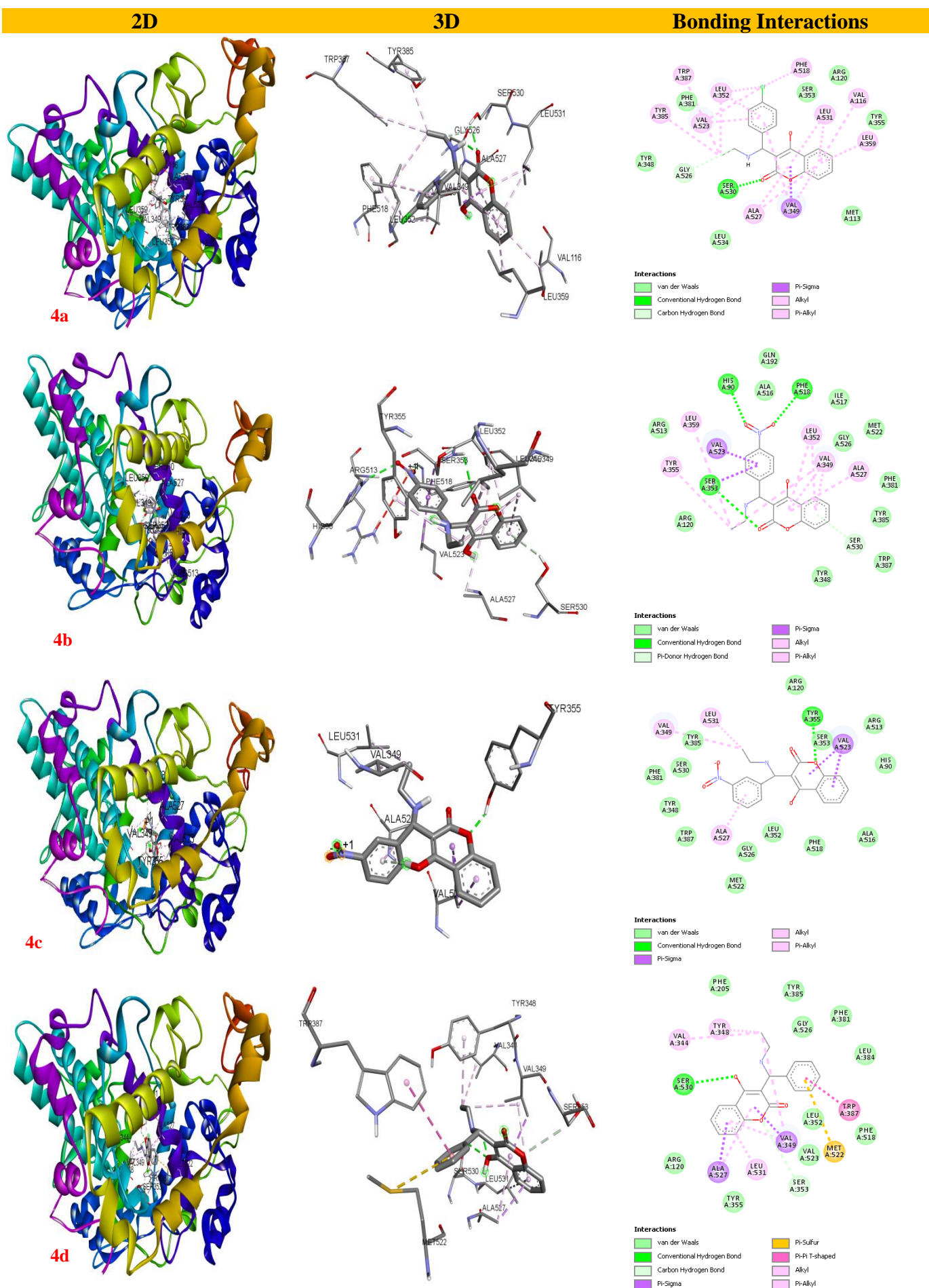


Fig. 7 Binding mode and visual interaction of designed ligands with 1PXX (4(a-d))

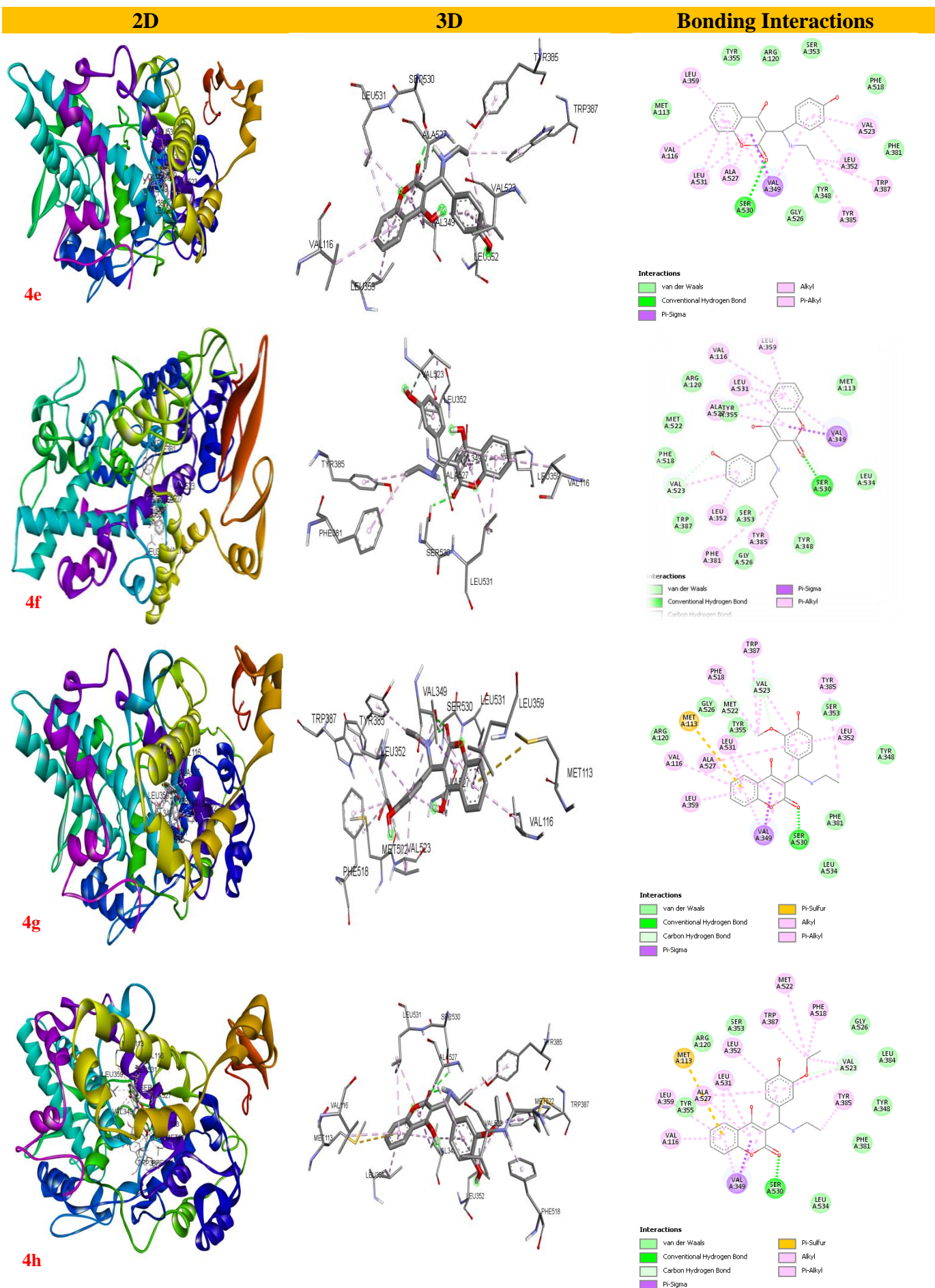


Fig. 8 Binding mode and visual interaction of designed ligands with 1PXX (4(e-h))

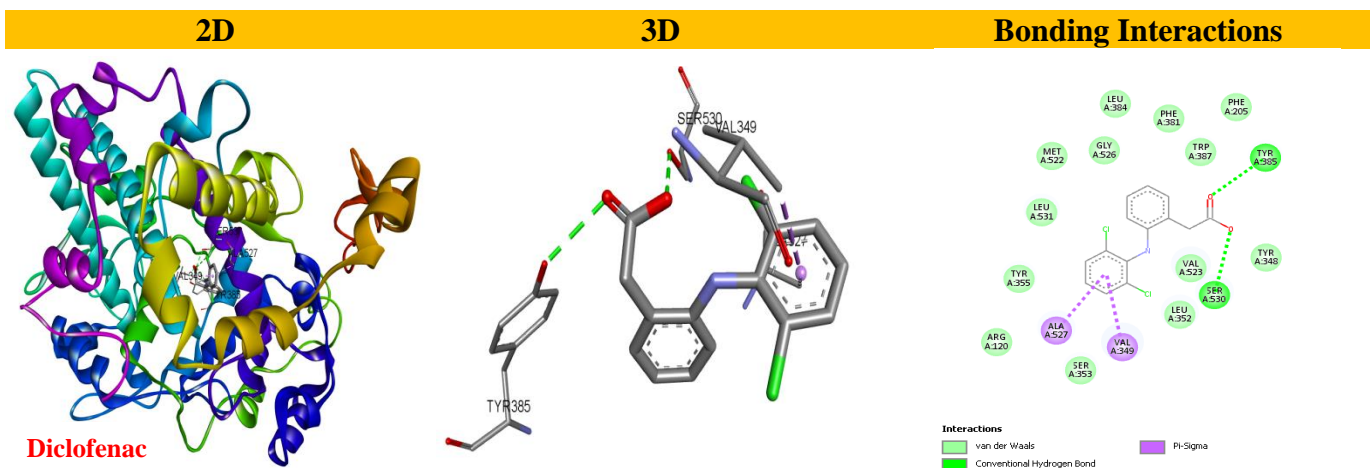


Fig. 9 Binding mode and visual interaction of designed ligands with 1PXX (Diclofenac)

4. Applications

4.1. Biological studies

4.1.1. Antioxidant study

The DPPH free radical scavenging activity of synthesized compounds **4(a-h)** was investigated according to the reported method with suitable modification [41–43]. DPPH (0.004%) in 95% of methanol was used for the preparation of a stock solution of synthesized compounds (1 mg/mL). The freshly prepared methanolic solution of DPPH was taken in the test tube and the stock solution was added (100 µg) to each test tube so that the ultimate volume will be 3mL. After 10 min, the absorbance was recorded using a spectrophotometer at 517 nm. Ascorbic acid (AA) was used as a reference standard and control sample having the same volume with no stock solution. The experiment was performed thrice and the IC₅₀ values are exhibited in Table 12. Fig. 11 represents the plot of IC₅₀ values of synthesized compounds. The DPPH radical scavenging activity (%) has been calculated and expressed as:

$$\% \text{ Inhibition } (I) = (A_b - A_a/A_a) \cdot 100, \quad (3)$$

where A_b – absorbance of blank (DPPH solution with no test sample), and A_a – absorbance due to sample (DPPH solution with test sample).

From the results, it was revealed that compounds **4h**, **4g** and **4f** with the lowest IC₅₀ value of 78, 81 and 89 µg/mL showed excellent scavenging activity, followed by the compounds **4d** and **4e** that exhibited noteworthy action with IC₅₀ values 96 and 112 µg/mL, respectively.

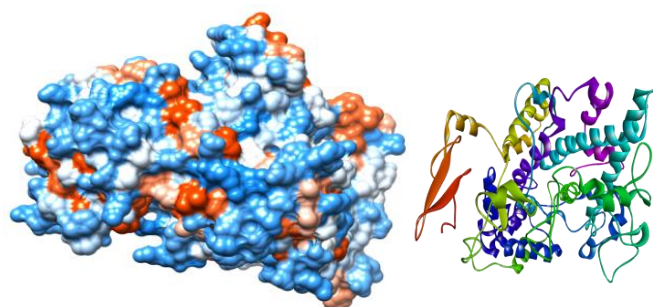


Fig. 10 Structure of Cyclooxygenase cox-2

Table 12 Antioxidant activity results of the synthesized compounds **4(a-h)**

Compounds	IC ₅₀ Values (µg/mL)
4a	141
4b	137
4c	198
4d	96
4e	112
4f	89
4g	81
4h	78
Ascorbic acid	118.29

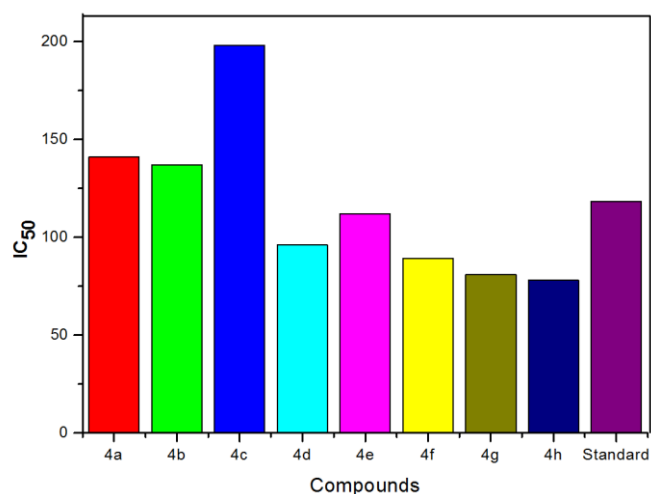


Fig. 11 Antioxidant activity results of the synthesized compounds **4(a-h)**

The compounds **4a**, **4b** and **4c**, showed comparably less stress-reducing activity with the IC₅₀ values 137 and 141 respectively. The compound **4c** showed the least scavenging activity with an IC₅₀ value of 198 µg/mL. The compounds **4d**, **4e**, **4f**, **4g** and **4h** exhibited more scavenging activity than the standard ascorbic acid. From Table 12, it can be concluded that compounds with an electron-donating group possess greater scavenging activity with less IC₅₀ values than compounds with an electron-withdrawing group of high IC₅₀ values.

4.2. Corrosion studies

4.2.1. Weight loss technique

The mild steel specimens (sheet) of compositions of 0.41% C, 0.46% Mn, 0.24% S, 0.22% Si, 0.17% Al and remaining is of Fe were used. The steel coupons of dimensions 5 cm×2 cm×0.2 cm were chosen for the weight loss experiment.

The test solution (1 M HCl) was prepared and a BAC (1 mM) was prepared using 1:50 (v/v) of DMSO/Millipore water. Different concentrations of BAC solutions (0.0, 0.001, 0.005, 0.01, 0.05, 0.1, and 1 mM) were prepared using 1 M HCl

4.2.2. Effect of concentration

Weight loss measurements were carried out by weighing MS specimens before and after their immersion in 100 mL of pure 1 M HCl and also having different amounts of BAC in 1 M HCl. All experiments were conducted at atmospheric ambient pressure and in the temperature range of 303–333 K. The corrosion rate (v_{corr}) and inhibition efficiency (IE) (η %) were calculated using the following equations 4 and 5, respectively.

$$v_{corr} = \frac{W_0 - W_1}{St}, \tag{4}$$

where W_0 is the weight loss value in the absence of BAC, W_1 is the weight loss value in the presence of BAC, S is the surface area of the MS specimen, t is the temperature. The corrosion rates (CR) were determined by using equation 5.

$$\eta\% = \frac{W_0 - W_1}{W_0} \cdot 100 \tag{5}$$

Among all the synthesized compounds **4e**, **4f** and **4h** exhibited superior IE, compounds **4d** and **4g** showed reasonable IE, and compounds **4c**, **4b**, and **4a** exhibited the least IE against 1M HCl solution. From Table 13 it was concluded that among all the synthesized compounds, those with electron-donating groups on the aromatic ring show the exceedingly superior corrosion inhibition property than compounds with electron-withdrawing groups on the aromatic ring [44], which is depicted in Fig. 12.

4.2.3. Effect of temperature

A study of the corrosion IE of synthesized compounds on MS in acid solutions of the synthesized compounds at different temperatures (303, 313, and 323 K) indicated that IE is better at lower temperature and decreases with temperature, as shown in Fig. 13. The decrease in IE with a rise in temperature is indicative of physisorption, which could be attributed to the gradual desorption of the adsorbed synthesized compounds from the surface of the metal [45, 46].

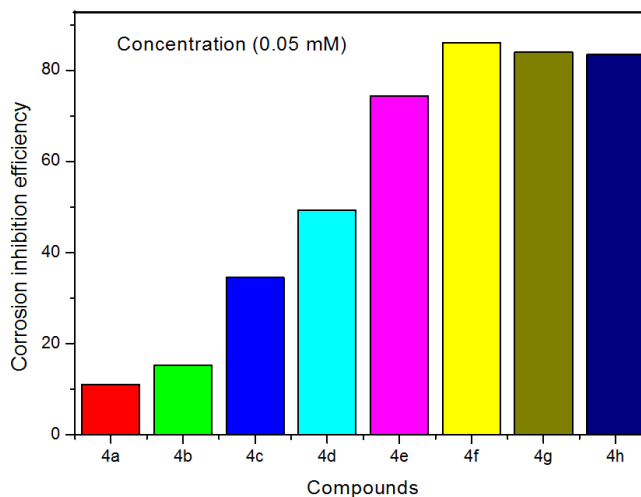


Fig. 12 Corrosion inhibition efficiency of the synthesized compounds

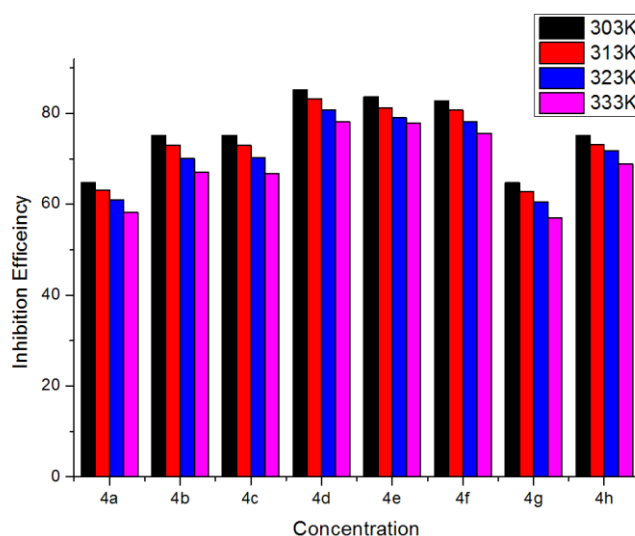


Fig. 13 Influences of temperatures on corrosion efficiencies of BAC at fixed time

Table 13 Corrosion inhibition efficiency of the synthesized compounds **4(a-h)**

Compounds	Weight in gram			Corrosion rate gram/day	Inhibition efficiency (IE)
	Initial W_1	Final W_2	Difference ΔW		
4a	3.9750	3.3782	0.4968	0.0001295	11.12
4b	3.7793	3.3060	0.4733	0.0017854	15.33
4c	3.7858	3.4200	0.3658	0.004025	34.56
4d	3.6377	3.3550	0.2827	0.005756	49.42
4e	3.8048	3.3891	0.4157	0.0086604	74.36
4f	3.7195	3.2383	0.4812	0.0100250	86.08
4g	3.8651	3.3954	0.4697	0.0097854	84.02
4h	3.8738	3.4073	0.4665	0.0097187	83.45
Blank	3.9000	3.3410	0.5590	-	-

5. Recyclability of the catalyst

The recyclability of the catalyst tests was performed to ensure the principle of green chemistry. The recycled catalyst used 6 times without any treatment and no appreciable loss in its catalytic activity was observed up to the sixth run (92%), which is demonstrated in Fig. 14.

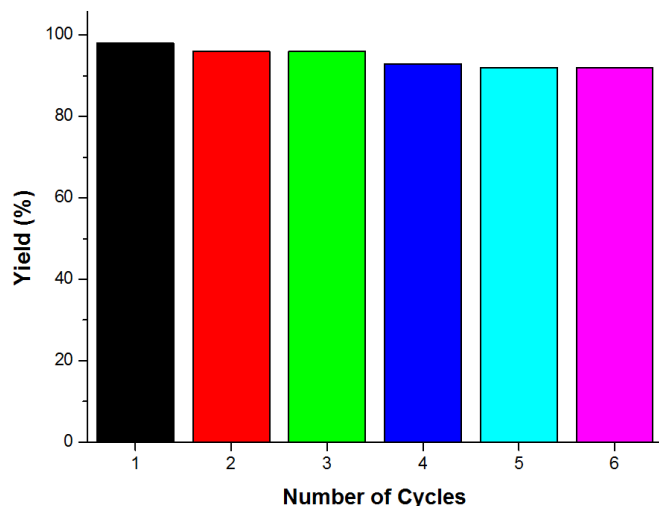


Fig. 14 Recyclability of the catalyst

6. Conclusions

We reported the novel synthesis of 3-[(ethylamino) (phenyl) methyl]-4-hydroxy-2H-chromen-2-one derivatives using biogenic ZnO NPs as a catalyst. Further, the structures of synthesized compounds were elucidated by different spectroscopic techniques. Absorption studies revealed that a bathochromic shift was observed in all the studied compounds. The ADMET studies revealed that all the compounds have drug likeliness properties, and *in silico* molecular docking studies revealed a good docking score of studied compounds with respect to cyclooxygenase cox-2. All the studied compounds exhibited superior antioxidant activity against ascorbic acid as standard. The corrosion study revealed that the new BAC functioned as a good corrosion inhibitor for MS in 1 M HCl solution. Furthermore, the recycled catalyst exhibited better catalytic activity up to the sixth run.

Acknowledgment

The authors are thankful to the Chairman, Department of Chemistry, Kuvempu University Shankaraghatta for providing the laboratory facilities and to the University of Mysore and Saif Karnatak University, Dharwad for providing spectra. One of the authors, Anjan Kumar G C thankful to the Council of Scientific and Industrial Research (CSIR), New Delhi, India, for providing a Junior Research fellowship [09/908(0010)/2019-EMR-I].

Conflicts of interest

The authors declare that there are no conflicts of interests regarding the publication of this work.

References

- Brahmachari G. Room temperature one-pot green synthesis of coumarin-3- carboxylic acids in water: a practical method for the large-scale synthesis. *ACS Sustain Chem Eng.* 2015;3:2350–2358. doi:[10.1021/acssuschemeng.5b00826](https://doi.org/10.1021/acssuschemeng.5b00826)
- Insuasty D, Castillo J, Becerra D, Rojas H, Abonia R. Synthesis of Biologically Active Molecules through Multicomponent Reactions. *Mol.* 2020;25:505. doi:[10.3390/molecules25030505](https://doi.org/10.3390/molecules25030505)
- Slobbe P, Ruijter E, Orru RVA. Recent applications of multicomponent reactions in medicinal chemistry. *Med Chem Comm.* 2012;3:1189. doi:[10.1039/c2md20089a](https://doi.org/10.1039/c2md20089a)
- Rao P, Konda S, Iqbal J, Oruganti S. InCl₃ catalyzed three-component synthesis of a-benzylamino coumarins and diketones. *Tetrahedron Lett.* 2012;53:5314–5317. doi:[10.1016/j.tetlet.2012.07.098](https://doi.org/10.1016/j.tetlet.2012.07.098)
- Kumar A, Kumar Gupta M, Kumar M. An efficient non-ionic surfactant catalyzed multicomponent synthesis of novel benzylamino coumarin derivative via Mannich type reaction in aqueous media. *Tetrahedron Lett.* 2011;52:4521–4525. doi:[10.1016/j.tetlet.2011.06.040](https://doi.org/10.1016/j.tetlet.2011.06.040)
- Alinasab Amiri A, Javanshir S, Dolatkah Z, Dekamin MG. SO₃H-Functionalized Mesoporous Silica Materials as Solid Acid Catalyst for Facile and Solvent-free Synthesis of 2H-Indazolo [2, 1-b] phthalazine-1, 6, 11-trione derivatives. *New J Chem.* 2015;39:9665–9671. doi:[10.1039/C5NJ01733E](https://doi.org/10.1039/C5NJ01733E)
- El-Helw EAE, Sallam HA, Elgubbi AS. Antioxidant activity of some N-heterocycles derived from 2-(1-(2-oxo-2H-chromen-3-yl) ethylidene) hydrazinecarbothioamide. *Synth Comm.* 2019;49(20):2651–2661. doi:[10.1080/00397911.2019.1638938](https://doi.org/10.1080/00397911.2019.1638938)
- Chen C-M, Chen W-L, Yang S-T, Lin T-H, Yang S-M, et al. New Synthetic 3-Benzoyl-5-Hydroxy-2H-Chromen-2-One (LM-031) inhibits polyglutamine aggregation and promotes neurite outgrowth through enhancement of CREB, NRF2, and Reduction of AMPK α in SCA17 cell models. *Oxid Med Cell Longev.* 2020;3129497. doi:[10.1155/2020/3129497](https://doi.org/10.1155/2020/3129497)
- Qin H-L, Zhang Z-W, Ravindar L, Rakesh KP. Antibacterial activities with the structure-activity relationship of coumarin derivatives. *Eur J Med Chem.* 2020;207:112832. doi:[10.1016/j.ejmech.2020.112832](https://doi.org/10.1016/j.ejmech.2020.112832)
- Hosseinzadegan S, Hazeri N, Maghsoodlou MT. Synthesis and evaluation of antimicrobial and antioxidant activity of novel 7-Aryl-6H, 7H- benzo[f] chromeno [4, 3-b] chromen-6-one by MgO nanoparticle as green catalyst. *J Heterocycl Chem.* 2019;1–6. doi:[10.1002/jhet.3796](https://doi.org/10.1002/jhet.3796)
- Khdhiri E, Mnafigui K, Ncir M, Feriani A, Ghazouani L, et al. Cardioprotective capacity of a novel (E)-N'-(1-(7-methoxy-2-oxo-2H-chromen-3-yl) ethylidene)-4-methylbenzenesulfonohydrazide against isoproterenol-induced myocardial infarction by moderating biochemical, oxidative stress, and histological parameters. *J Biochem Mol Toxicol.* 2021;22747. doi:[10.1002/jbt.22747](https://doi.org/10.1002/jbt.22747)
- Ali A, Ali A, Bakht MA, Ahsan MJ. Ultrasound promoted synthesis of N-(substituted phenyl)-2-(7- hydroxy-4-methyl-2H-chromen-2-ylidene) hydrazine-1-carboxamides as cytotoxic and antioxidant agents. *J Mol Struct.* 2021;1238:130452. doi:[10.1016/j.molstruc.2021.130452](https://doi.org/10.1016/j.molstruc.2021.130452)
- Bensalah D, Mnasri A, Chakchouk-Mtibaa A, Mansour L, Mellouli L, Hamdi N. Synthesis and antioxidant properties of some new thiazolyl coumarin derivatives. *Green Chem Lett Rev.* 2020;13(2):155–163. doi:[10.1080/17518253.2020.1762935](https://doi.org/10.1080/17518253.2020.1762935)
- Alshib HM, Al-Abdullah ES, Haiba ME, Alkahtani HM, Awad GEA, et al. Synthesis and evaluation of new coumarin derivatives as antioxidant, antimicrobial, and anti-inflammatory agents. *Mol.* 2020;25:3251. doi:[10.3390/molecules25143251](https://doi.org/10.3390/molecules25143251)

15. Bansal Y, Sethi P, Bansal G. Coumarin: a potential nucleus for anti-inflammatory molecules. *Med Chem Res.* 2013;22:3049–3060. doi:[10.1007/s00044-012-0321-6](https://doi.org/10.1007/s00044-012-0321-6)
16. Nagaraja O, Bodke YD, Pushpavathi I, Ravi Kumar S. Synthesis, characterization and biological investigations of potentially bioactive heterocyclic compounds containing 4-hydroxy coumarin. *Heliyon.* 2020;6:e042452. doi:[10.1016/j.heliyon.2020.e04245](https://doi.org/10.1016/j.heliyon.2020.e04245)
17. Kerru N, Gummidi L, Maddila S, Gangu KK, Jonnalagadda SB. A review on recent advances in nitrogen-containing molecules and their biological applications. *Mol.* 2020;25:1909. doi:[10.3390/molecules25081909](https://doi.org/10.3390/molecules25081909)
18. Kamal LC, Sethuraman MG. Opuntia: an active principle of opuntia elatior as an eco-friendly inhibitor of corrosion of mild steel in acid medium. *ACS Sustain Chem Eng.* 2014;2:606–613. doi:[10.1021/sc4003642](https://doi.org/10.1021/sc4003642)
19. Gopal J. Priyanka dwivedi, shanthi sundaram and rajiv prakash. Inhibitive effect of chlorophytum borivilianum root extract on mild steel corrosion in HCl and H₂SO₄ solutions. *Ind Eng Chem Res.* 2013;52:10673–10681. doi:[10.1021/ie4008387](https://doi.org/10.1021/ie4008387)
20. Al-Amiery AA, Al-Majedy YK, Kadhum AAH, Mohamad AB. New coumarin derivative as an eco-friendly inhibitor of corrosion of mild steel in acid medium. *Mol.* 2015;20:366–383. doi:[10.3390/molecules20010366](https://doi.org/10.3390/molecules20010366)
21. Singh AK, Shukla SK, Quraishi MA, Ebenso EE. Investigation of adsorption characteristics of N, N-[(methylimino)dimethylidene] di-2,4-xylidine as corrosion inhibitor at mild steel/sulphuric acid interface. *J Taiwan Inst Chem Eng.* 2012;43:463–472. doi:[10.1016/j.jtice.2011.10.012](https://doi.org/10.1016/j.jtice.2011.10.012)
22. Ghosh PP, Das AR. Nano crystalline ZnO: a competent and reusable catalyst for one pot synthesis of novel benzylamino coumarin derivatives in aqueous media. *Tetrahedron Lett.* 2012;53:3140–3143. doi:[10.1016/j.tetlet.2012.04.033](https://doi.org/10.1016/j.tetlet.2012.04.033)
23. Viradiya DJ, Kotadiya VC, Khunt MD, Baria BH, Bhoya UC. PEG mediated eco-friendly one pot synthesis of benzylamine coumarin derivatives using multicomponent reactant. *Int Lett Chem Phys Astron.* 2014;11(2):177–184.
24. Cao B, Liu R, Huang ZX, Ge S. Flash synthesis of flower-like ZnO nanostructures by microwave-induced combustion process. *Mater Lett.* 2011;65:160–163. doi:[10.1016/j.matlet.2010.09.072](https://doi.org/10.1016/j.matlet.2010.09.072)
25. Kumar B, Smita K, Cumbal L, Debut A. Green approach for fabrication and applications of zinc oxide nanoparticles. *Bioinorg Chem Appl.* 2014;523869. doi:[10.1155/2014/523869](https://doi.org/10.1155/2014/523869)
26. Banerjee B. Recent developments on nano ZnO catalyzed synthesis of bioactive heterocycles. *J Nanostruct Chem.* 2017;7:389–413. doi:[10.1007/s40097-017-0247-0](https://doi.org/10.1007/s40097-017-0247-0)
27. Molinspiration Cheminformatics. Available from: <http://www.molinspiration.com/>
28. ADMETlab. Available from: <http://admet.scbdd.com/>
29. Shwetha UR, Rajith Kumar CR, Kiran MS, Virupaxappa S, Betageri, Latha MS, et. al. Biogenic synthesis of NiO nanoparticles using areca catechu leaf extract and their antidiabetic and cytotoxic effects. *Mol.* 2021;26(9):2448. doi:[10.3390/molecules26092448](https://doi.org/10.3390/molecules26092448)
30. Lipinski CA. Lead- and drug-like compounds: the rule-of-five revolution. *Drug Discovery Today: Technol.* 2004;1(4):337–341. doi:[10.1016/j.ddtec.2004.11.007](https://doi.org/10.1016/j.ddtec.2004.11.007)
31. Manjunatha KS, Satyanarayan ND, Kaviraj MY, Adarsha HJ. Anti-proliferative and ADMET screening of novel 3-(1H-indol-3-yl)-1, 3-diphenylpropan-1-one derivatives: *Cogent Chem.* 2016;2(1):1172542. doi:[10.1080/23312009.2016.1172542](https://doi.org/10.1080/23312009.2016.1172542)
32. Shatokhin SS, Tuskaev VA, Gagieva Sch, Ybalkina EYu, et.al. Synthesis, structural characterization, antioxidant and cytotoxic activity towards human cancer cell lines and computational studies of new Ni(II), Co(II) and Pd(II) complexes with 3-[bis(3,5-dimethylpyrazol-1-yl)methyl]chromen-4-one derivatives. *J Mol Struct.* 2021. doi:[10.1016/j.molstruc.2021.130706](https://doi.org/10.1016/j.molstruc.2021.130706)
33. Kara J, Suwanhom P, Wattanapiromsakul C, Nualnoi T, Puripattanavong J, et.al. Synthesis of 2-(2-oxo-2H-chromen-4-yl) acetamides as potent acetylcholinesterase inhibitors and molecular insights into binding interactions. *Chem Life Sci.* 2019;1800310. doi:[10.1002/ardp.201800310](https://doi.org/10.1002/ardp.201800310)
34. Dong J, Wang N-N, Yao Z-J. ADMETlab: a platform for systematic ADMET evaluation based on a comprehensively collected ADMET database. *J Chem.* 2018;10. doi:[10.1186/s13321-018-0283-x](https://doi.org/10.1186/s13321-018-0283-x)
35. Rowlinson SW, Kiefer JR, Prusakiewicz JJ, Pawlitz JL, Kozak KR, Kalgutkar AS, Stallings WC, Kurumbail RG, Marnett LJ. A Novel mechanism of cyclooxygenase-2 inhibition involving interactions with Ser-530 and Tyr-385. *J Biol Chem.* 2003;278:45763–45769. doi:[10.1074/jbc.M305481200](https://doi.org/10.1074/jbc.M305481200)
36. RCSB PDB. Available from: <https://www.rcsb.org>
37. Gaillard T. Evaluation of *AutoDock* and *AutoDock Vina* on the CASF-2013 Benchmark. *J Chem Inf Model.* 2018;58:1697–1706. doi:[10.1021/acs.jcim.8b00312](https://doi.org/10.1021/acs.jcim.8b00312)
38. Bhowmik D, Sharma RD, Prakash A, Kumar D. Identification of nafamostat and VR23 as COVID-19 drug candidates by targeting 3CLpro and PLpro. *J Mol Struct.* 2021;1233:130094. doi:[10.1016/j.molstruc.2021.130094](https://doi.org/10.1016/j.molstruc.2021.130094)
39. Pettersen EF, Goddard TD, Huang CC, Couch GS, Greenblatt DM, Meng EC, Ferrin TE. A visualization system for exploratory research and analysis. *J Comput Chem.* 2004;25(13):1605–1612. doi:[10.1002/jcc.20084](https://doi.org/10.1002/jcc.20084)
40. Pradeep P, Archana Y, Laxman B, Nippu BN, Satyanarayan ND, Anand M, Akshay G, Shankar H, Sandeep S. [MerDABCO-SO₃H]Cl catalyzed synthesis, antimicrobial and antioxidant evaluation and molecular docking study of pyrazolopyranopyrimidines. *J Mol Struct.* 2021;1242:130672. doi:[10.1016/j.molstruc.2021.130672](https://doi.org/10.1016/j.molstruc.2021.130672)
41. Sahar A, Khan ZA, Ahmad M, Zahoor AF, Mansha A, et.al. Synthesis and antioxidant potential of some biscoumarin derivatives. *Tropical J Pharm Res.* 2017;16(1):203–210. doi:[10.4314/tjpr.v16i1.27](https://doi.org/10.4314/tjpr.v16i1.27)
42. Nagaraja O, Bodke YD, Kenchappa R, Ravi Kumar S. Synthesis and characterization of 3-[3-(1H-benzimidazol-2-ylsulfanyl)-3-phenyl propanoyl]-2H-chromen-2-one derivatives as potential biological agents. *Chem Data Collect.* 2020;27:100369. doi:[10.1016/j.cdc.2020.100369](https://doi.org/10.1016/j.cdc.2020.100369)
43. Yasar Q, Zaheer Z. 4-aminoantipyrene analogs as anti-inflammatory and antioxidant agents: synthesis, biological evaluation and molecular docking studies. *Int J Pharm Investig.* 2021;11(1):14–22. doi:[10.5530/ijpi.2021.1.4](https://doi.org/10.5530/ijpi.2021.1.4)
44. Al-Azawi KF, Al-Baghdadi SB, Mohamed AZ, Al-Amiery AA, Abed TK, Mohammed SA, et. al. Synthesis, inhibition effects and quantum chemical studies of a novel coumarin derivative on the corrosion of mild steel in a hydrochloric acid solution. *Chem Cent J.* 2016;10:23. doi:[10.1186/s13065-016-0170-3](https://doi.org/10.1186/s13065-016-0170-3)
45. Abdallah M, Zaafarany IA, Foudaand AS, El-Nagar W. Coumarin Derivatives as Corrosion Inhibitors for Zinc in HCl Solutions. *J Electrochem Plat Technol.* 2014. doi:[10.12850/ISSN2196-0267.JEPT3190](https://doi.org/10.12850/ISSN2196-0267.JEPT3190)
46. Vinutha MR, Venkatesha TV, Nagaraja C. Anticorrosive ability of electrochemically synthesized 2, 2'-disulfanediylaniline for mild steel corrosion: electrochemical and thermodynamic studies. *Int J Ind Chem.* 2018;9:185–197. doi:[10.1007/s40090-018-0149-0](https://doi.org/10.1007/s40090-018-0149-0)